Macromolecules 1994, *27*, 5377–5381

A Theoretical Study of Tacticity Effects on Poly(vinyl chloride)/ Poly(methyl methacrylate) Miscibility

J. D. Honeycutt[†]

BIOSYM Technologies, Inc., 9685 Scranton Road, San Diego, California 92121

Received January 28, 1994; Revised Manuscript Received June 20, 1994[⊛]

ABSTRACT: The polymer reference interaction site model (PRISM) theory is applied to the study of tacticity effects in blends of poly(vinyl chloride) (PVC) and poly(methyl methacrylate) (PMMA). The single-chain structure factors required as input to the theory are computed using Monte Carlo simulations based on rotational isomeric state (RIS) statistical weights. The PRISM results agree with the observed experimental trends for the systems where data are available. The observed and predicted trends appear to arise from a competition between effects due to local conformations and those due to overall chain stiffness.

Introduction

Blending or alloying of polymers is a method of producing desirable materials without the effort of devising new syntheses. Discovering miscible blends can be difficult, however, for two reasons: (1) unlike small molecules, polymers tend not to mix, and (2) whether two polymers do mix is determined by a subtle balance of competing factors. Even a slight modification of one polymer in a miscible pair may render the pair immiscible. Consequently, the search for new blends often involves a great deal of trial and error, due to the difficulty of treating such subtle effects theoretically. This paper describes an approach for modeling one of the these effects: the influence of tacticity.

It is known experimentally that poly(methyl methacrylate) (PMMA) varies greatly in its miscibility with poly(vinyl chloride) (PVC) and related polymers (Saran and chlorinated PVC) according to the tacticity of the PMMA.[1–5] Tacticity effects have also been observed in phase diagrams of poly(ethyl methacrylate) mixed with poly(vinylidene fluoride) (PVDF). Blends of PMMA and PVDF phase separate at high temperatures,[6] but because of thermal decomposition of the PMMA it has not been possible to directly determined the effect of PMMA tacticity on the miscibility of this system. Measurements of melting point depression, however, indicate that isotactic PMMA (it-PMMA) interacts more strongly with PVDF than does syndiotactic PMMA (st-PMMA).[7] Tacticity effects have been seen in polystyrene/poly(vinyl methyl ether) blends as well.[8]

These effects have variously been explained as due to differences in chain conformation with tacticity,[1,3,5] to equation of state contributions,[3,9] to differences in interaction energies,[4] and to changes in chain conformation upon blending.[10] These different explanations are not necessarily inconsistent with each other. For example, the equation of state theories,[11] based on thermodynamics, leave open the issue of the microscopic causes of the effects they describe. The purpose of this study is to probe the molecular origin of tacticity effects on blend miscibility using the PRISM theory of polymer blends. The systems studied are PVC/PMMA blends, for which unambiguous experimental phase data exist.

The polymer reference interaction site model (PRISM) theory is an off-lattice integral equation theory able to account for chemical detail in predicting the structural and thermodynamic properties of polymer systems in the liquid state.[12–15] A PRISM calculation takes as input the single-chain structure factor, $\hat{\omega}(\mathbf{k})$, of each component of the system. This function is the Fourier transform of the intramolecular pair distribution function and may be computed using Monte Carlo simulations based on rotational isomeric state (RIS) theory.[16] In using this information, PRISM theory is able to capture the effect of chain microstructure, including tacticity, on miscibility behavior. In this study, it is in the single-chain structure factor that the effects of tacticity are directly manifested, in that the tacticity of a vinyl chain has a great effect on the distribution of conformations that the chain adopts.

Theory

PRISM theory is treated extensively elsewhere[12–15] and will only be summarized here. In the PRISM picture, a polymer molecule is represented as a set of connected *interaction sites*, each site being an atom or small group of atoms. The sites are understood to interact with sites on other molecules through spherically symmetric potentials. In this investigation, these are hard core potentials with Lennard-Jones tails:

$$u_{\alpha\beta}(r) = \infty, \qquad r < \sigma_{\alpha\beta} \tag{1a}$$

$$u_{\alpha\beta}(r) = \epsilon_{\alpha\beta}\left[\left(\frac{\sigma_{\alpha\beta}}{r}\right)^{12} - 2\left(\frac{\sigma_{\alpha\beta}}{r}\right)^{6}\right], \qquad r > \sigma_{\alpha\beta} \tag{1b}$$

Here, α and β refer to site types; $\epsilon_{\alpha\beta}$ is the Lennard-Jones well depth, and $\sigma_{\alpha\beta}$ is the hard core diameter.

The theory is based on the site–site Ornstein–Zernike (OZ) equation of Chandler and Andersen[17] for molecular systems in the liquid state:

$$\mathbf{H}(r) = \int \mathrm{d}\mathbf{r}' \int \mathrm{d}\mathbf{r}''\, \boldsymbol{\Omega}(|\mathbf{r}-\mathbf{r}'|)\, \mathbf{C}(|\mathbf{r}'-\mathbf{r}''|)\, [\boldsymbol{\Omega}(r'') + \mathbf{H}(r'')] \tag{2}$$

Here, $\mathbf{H}(r)$ is the matrix of intermolecular site–site pair correlation functions for all possible pairs of site types; $\mathbf{C}(r)$ is the corresponding matrix of direct correlation functions, and $\boldsymbol{\Omega}(r)$ is the matrix of *intra*molecular site–site distribution functions. Note that, because the elements of the above equation are matrices, it in general represents a *set* of coupled integral equations.

In eq 2, the site and molecular densities have been adsorbed into the various matrices. The elements of $\mathbf{H}(r)$ are $\rho_\alpha\rho_\beta h_{\alpha\beta}(r)$. The elements of $\boldsymbol{\Omega}(r)$ are $\tilde{\rho}_i\omega_{\alpha\beta}(r)$ for sites α and β in the same chain (chain i) and zero for α and β in different chains. The elements of $\mathbf{C}(r)$ are simply $c_{\alpha\beta}(r)$, the site–site direct correction functions. Here, ρ_α

[†] E-mail dana@biosym.com.

[⊛] Abstract published in *Advance ACS Abstracts,* August 1, 1994.

0024-9297/94/2227-5377$04.50/0

and ρ_β refer to the number densities of sites α and β, and $\tilde{\rho}_i$ refers to the number density of sites of all types contained in chain i.

It is through the $\mathbf{\Omega}(r)$ matrix that the single-molecule structure enters the OZ equation. The definition of the partial intramolecular distribution functions, $\omega_{\alpha\beta}(r)$, is as follows:

$$\omega_{\alpha\beta}(r) = \left\langle \frac{1}{N_i} \sum_{j\in\{\alpha\}} \sum_{k\in\{\beta\}} \delta(\mathbf{r}-\mathbf{r}_{jk}) \right\rangle \qquad (3)$$

Here, the expressions $j \in \{\alpha\}$ and $k \in \{\beta\}$ indicate that the subscript j is summed over all sites of type α and that k is summed over all sites of type β. N_i is the number of sites in chain i, the chain in which sites of type α and β occur. (For α and β in different chains, $\omega_{\alpha\beta}(r)$ is zero.) The meaning of the term "site type" is discussed below. The angle brackets in eq 3 indicate a Boltzmann average over all conformations. A rotational isomeric state (RIS) Monte Carlo scheme is used in this study to perform this average.

In PRISM theory, two sites are equivalent (of the same type) if their direct correlation functions with all other sites are equal to each other. That is, sites j and k are equivalent if $c_{jl}(r) = c_{kl}(r)$ for all sites l. For a linear polymer chain whose degree of polymerization (or number of sites) is N, there are $N/2$ chemically distinct sites and thus in principle $N/2$ site types. Treating these sites as distinct within the OZ equation would make the equation insoluble for practical purposes—it would require solving of order N^2 coupled integral equations. However, in a long polymer chain, sites away from the ends experience environments very similar to each other and may be treated as equivalent. If explicit end effects are neglected, the number of site types may be greatly reduced, down to the number of *locally* chemically distinct sites in the body of the chain.[14] This is the approximation that renders PRISM theory tractable and has been shown empirically—by comparison to simulations and experiments—to be a good one.[18]

While the OZ equation may be regarded as exact, as *defining* the site–site direct correlation functions, by itself it is a single equation with two unknowns ($\mathbf{H}(r)$ and $\mathbf{C}(r)$). (On an element-by-element basis, it represents $n(n+1)/2$ equations with $2n(n+1)/2$ unknowns, where n is the number of site types.) An additional closure relation is required to solve the OZ equation in an approximate manner. The mean spherical approximation (MSA) closure is used here:

$$h_{\alpha\beta}(r) = -1, \qquad r < \sigma_{\alpha\beta} \qquad (4a)$$

$$c_{\alpha\beta}(r) = -u_{\alpha\beta}(r)/k_{\mathrm{B}}T, \qquad r > \sigma_{\alpha\beta} \qquad (4b)$$

This closure, used in most early PRISM work,[12-15,18] appears to treat packing effects well in systems with hard sphere site–site interactions.[18] (For such systems, the MSA is equivalent to the Percus–Yevick closure.) When treating blend systems with soft potential tails, the MSA is known to have deficiencies. In particular, it is qualitatively wrong in its predictions of the effect of molecular weight on miscibility and therefore quantitatively incorrect for predicting miscibility of model systems at any particular molecular weight.[19-21] However, the MSA was deemed adequate for this study for two reasons: (1) This study is concerned with trends as tacticity is changed at fixed molecular weight rather than with obtaining quantitatively accurate phase diagrams. (2) The effects studied here are essentially packing effects, which are dominated by hard core interactions, for which the MSA is suitable. More sophisticated closures have been derived and have been shown to be more accurate than the MSA for model systems displaying upper critical solution temperature (UCST) phase diagrams.[21] The use of these so-called "molecular closures" requires that the hard core "reference system" and the potential tail contributions to the structure be treated separately. However, it is unclear whether the particular method used in this study to produce phase diagrams with lower critical solution temperatures (LCSTs)[22] can be used with these more sophisticated closures. (The hard-core reference system is phase-separated in this case.)

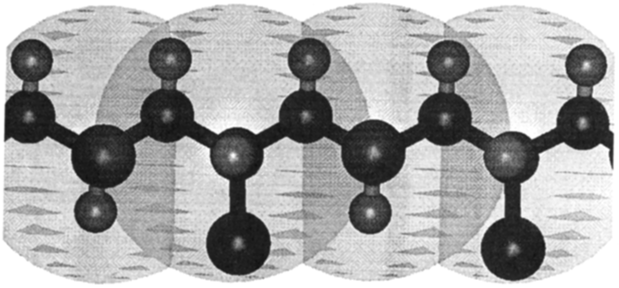

Figure 1. Segment of a PVC chain illustrating the site representation used in this study. The sites are centered at the α-carbon atoms and have a hard core diameter of 4.93 Å, as illustrated by the large spheres in the figure.

To solve the OZ equation, it is convenient to work in Fourier space, in which the equation is simply an algebraic relation:

$$\hat{\mathbf{H}}(k) = \hat{\mathbf{\Omega}}(k)\,\hat{\mathbf{C}}(k)[\hat{\mathbf{\Omega}}(k) + \hat{\mathbf{H}}(k)] \qquad (5)$$

where

$$\hat{\mathbf{H}}(k) \equiv \int \mathrm{d}\mathbf{r}\,\exp(-i\mathbf{k}\cdot\mathbf{r})\mathbf{H}(r) \qquad (6)$$

with similar definitions for $\hat{\mathbf{C}}(k)$ and $\hat{\mathbf{\Omega}}(k)$. The elements of $\hat{\mathbf{\Omega}}(k)$, $\tilde{\rho}_i\hat{\omega}_{\alpha\beta}(k)$, are the single-chain particle structure factors (multiplied by the density).

Given $\hat{\omega}_{\alpha\beta}(k)$ functions, potentials, and a closure, PRISM theory can be used to compute blend phase diagrams in the form of spinodal curves. Here, the variational method of Lowden and Chandler is used to solve the PRISM equations.[23] At a given system composition, the spinodal temperature is the temperature at which the zero wave vector partial (site–site) scattering functions diverge. By performing calculations over a range of compositions, the complete phase diagram (spinodal curve) can be mapped out.

PVC/PMMA Model and Parameters

For the PRISM calculations, each repeat unit on a PVC or PMMA chain is treated as a spherically symmetric site (Figure 1). Thus, the stereochemistry is not explicitly included in the site representation. However, it is taken into account in the single-chain RIS conformational statistics used as input to the PRISM calculation in that chains of differing tacticity have different statistical weights. Less coarse-grained site representations are possible but are computationally much more expensive than the one used here.

The $\sigma_{\alpha\beta}$ parameters for the monomer–monomer interactions are crude estimates based on the mean cross-sectional areas of the various repeat units, as computed by a group additivity method.[24] The $\epsilon_{\alpha\beta}$ parameters were chosen to give a specific attraction between unlike monomers. To keep the number of parameters small, the

Table 1. Site-Site (Monomer–Monomer) Potential Parameters Used in PRISM Calculations[a]

interaction	σ(Å)	ϵ/k_B (K)
VC–VC	4.93	0
MMA–MMA	6.92	0
VC–MMA	6.40	10.0

[a] VC, vinyl chloride; MMA, methyl methacrylate.

well depths for interactions between like monomers were set to zero. The $\sigma_{\alpha\beta}$ parameter for the interaction between unlike monomers was set to a value greater than the mean of the $\sigma_{\alpha\alpha}$ parameters for like monomers. This combination of parameters gives rise to phase diagrams of the LCST form, as long as $\sigma_{\alpha\beta}$ for unlike monomers is sufficiently large.[22] (For $\sigma_{\alpha\beta}$ below a certain value, which is still greater than the mean of $\sigma_{\alpha\alpha}$ values, the system is miscible at all temperatures.) At low temperatures, the attractive specific interactions dominate, and the system is miscible. At high temperatures, the hard core interactions dominate, leading to phase separation. Table 1 lists the values of the parameters used.

Apart from choosing interactions to yield critical temperatures in the 200–400 K range for the it-PVC systems, no attempt was made to optimize the potentials by fitting to experimental data. For this investigation it is the trend, not the absolute location of the coexistence curves, that is of interest. Once a set of potentials was chosen, it was used for *all* systems studied, irrespective of chain tacticity. Thus, *there is no bias in the potentials themselves that would favor miscibility of one microstructure over another.* Limited calculations were done for systems with slightly different potentials, yielding results qualitatively the same as those reported here.

For PMMA of all tacticities, a density of 1.19 g/cm^3 was used; for PVC, 1.39 g/cm^3.[27] Volume changes upon mixing were neglected.

For the RIS Monte Carlo calculations of the single-chain structure factors,[16] statistical weights were taken from the literature.[25,26] Chains containing 400 bonds each were used, corresponding to molecular weights of 12 500 for PVC and 20 000 for PMMA. Separate Monte Carlo calculations were performed for it-PMMA, st-PMMA, it-PVC, st-PVC, and at-PVC (50% meso diads).

In experimental studies, commercial grade PVC has typically been used. This PVC is atactic with approximately 45% meso diad content.[27] Because of its statistical nature, such a system is difficult to treat in a theory such as PRISM that incorporates chemical detail. As an approximation, the structure factors of chains with differing microstructure may be averaged together before performing PRISM computations, but it is not clear *a priori* the extent to which such "preaveraging" is valid in this context. Here, "preaveraging" indicates that the single-chain structure factors are averaged together to form the structure factor for an "effective atactic chain" *before* the PRISM calculation is performed. (This approximation amounts to treating the quenched randomness in the chains' stereosequences as annealed randomness.)

Alternatively, a separate PRISM calculation may be performed for each chain microstructure, but this is also an approximation. The real system contains PVC chains with many microstructures in equilibrium with stereoregular PMMA chains with a small number (for perfect stereoregularity, only one) of microstructures. This is quite different from stereoregular PMMA chains in equilibrium with "atactic" PVC chains of only a single microstructure, which is what this latter approximation represents.

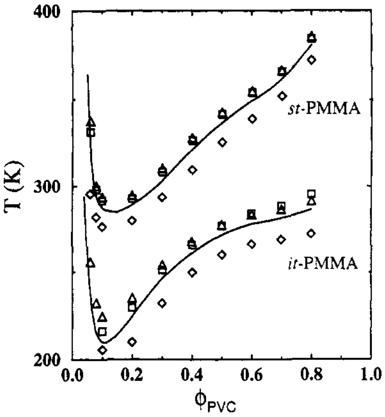

Figure 2. PRISM spinodal curves for it-PMMA and st-PMMA blended with at-PVC. Solid lines: at-PVC $\hat{\omega}(k)$ functions are averaged over three atactic microstructures. Symbols: $\hat{\omega}(k)$ functions are for distinct PVC microstructures.

For at-PVC, three randomly generated chains of differing stereochemical configuration were used. PRISM calculations were performed on blends with PMMA of each of these chains as well as a blend for which the structure factors of these three chains were "preaveraged" together and then used as input to the PRISM calculation. In a real melt of atactic chains, there are of course many more than three different stereochemical sequences, but even for only three microstructures, the scatter in the computed phase diagrams is not great (Figure 2). Also, the qualitative results are insensitive to the way the averaging over microstructure is done.

An implicit assumption in the PRISM calculations performed here is that the probable chain conformations in the melt do not change greatly when the system is blended. Self-consistent versions of PRISM theory have been formulated[28] that can account for the effect of the environment on a chain's conformation, but all calculations reported here use the non-self-consistent version of the theory.

Finally, PRISM theory is a theory of polymer liquids and does not itself predict a freezing or glass transition. Liquid–liquid spinodal curves calculated with PRISM theory may occur at temperatures at which the experimental system would be in the solid state. This study thus addresses only the issue of liquid–liquid miscibility.

Results and Discussion

The most straightforward case to treat computationally is that in which both components of the system are stereoregular. For this case, the constituent chains of each component all have identical stereochemical sequences; thus, there is no statistical distribution of sequences over which averaging must be done. Phase diagrams for stereoregular systems are shown in Figure 3 for it-PVC blended with either it-PMMA or st-PMMA and in Figure 4 for st-PVC blended with stereoregular PMMAs.

Experimentally, the tacticity of PVC cannot be controlled to the extent that it can for PMMA, and commodity PVC is atactic. Thus, it is Figure 2 for at-PVC that corresponds directly to the experimental situation.

A few general observations can be made concerning the phase diagrams in Figures 2–4. They reproduce the experimental trend that syndiotactic PMMA is more miscible with PVC than is isotactic PMMA. This occurs irrespective of the PVC tacticity, but the effect is more pronounced for isotactic PVC. Note that isotactic PVC is predicted to be more miscible with PMMA of either tacticity than is atactic or syndiotactic PVC. This is the

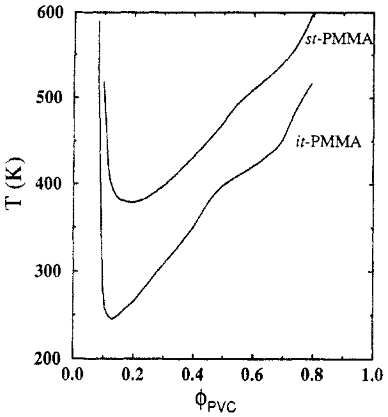

Figure 3. PRISM spinodal curves for it-PMMA and st-PMMA blended with it-PVC.

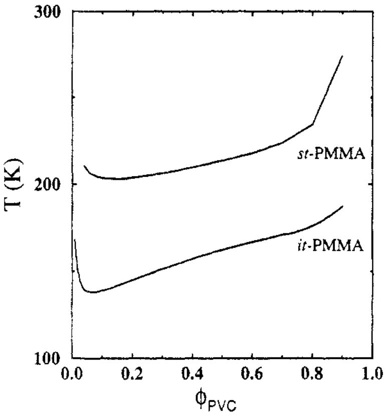

Figure 4. PRISM spinodal curves for it-PMMA and st-PMMA blended with st-PVC.

opposite of the trend in miscibility with respect to the PMMA tacticity. A tentative explanation for these opposite trends is given below. The predictions of the effect of PVC tacticity on the results cannot yet be confirmed or refuted experimentally, due to the current inability to synthesize stereoregular PVC.

The phase diagrams in Figures 2–4 are significantly more asymmetric than those seen experimentally,[3,5] even when molecular weight effects are taken into account.[29] This arises at least partially from the large difference in the monomer diameters for PVC and PMMA that were used in this study (Table 1) and indicates that the simple method used to estimate them is only qualitatively correct. Phase diagrams have also been computed with a less asymmetrical (but more *ad hoc*) set of hard core diameters. These are less skewed and do not alter the qualitative result that the syndiotactic PMMA is more miscible with PVC.

Figure 5 shows the characteristic ratio (C_n) of PVC and PMMA chains as a function of temperature, as calculated with standard RIS theory.[25,26,30] Because all of the chains are vinyl chains, the C_n values represent the mean square end-to-end distances normalized by the same numerical factor. No simple rule along the lines of, "Chains of similar C_n tend to mix better", is apparent from Figure 5 and the PRISM phase diagrams. The same is true if the RIS-computed persistence lengths for the various chains are compared to each other. The observed trends are due to causes more subtle than simple chain size effects.

It is possible to tentatively explain the PRISM results in terms of the characteristic ratios by first noting two facts.

(1) In the systems studied here, a specific attraction between the two components is present. Other things being equal, one expects such a system to be more miscible as the number of favorable site–site contacts between the two species increases. In the syndiotactic chains, the abundance of *trans* bonds is greater than for isotactic (or atactic) chains. This results in conformations that are locally more "open" and therefore more able to allow contacts with sites on other chains. An abundance of *gauche* states would lead to a more tightly coiled chain, with interchain contacts precluded to a large extent by interchain contacts.

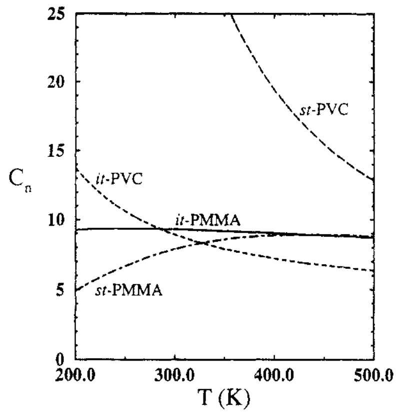

Figure 5. RIS-computed characteristic ratios (C_n) for the 200-mer chains used in this study.

(2) Another fact to note is that rigid-rod polymers and random coils tend not to be miscible, due to the entropic penalty for packing rods and coils together. Generally speaking, a greater abundance of *trans* bonds in a polymer backbone means a stiffer, more rodlike chain. However, in the case of st-PMMA, the two types of valence angle in the chain backbone have very different values (108 and 124°).[26] Consequently, long *trans* sequences form loops, giving rise to C_n values for st-PMMA that are smaller than or comparable to those for it-PMMA. This phenomenon does not occur in PVC, and Figure 5 shows that st-PVC becomes more and more rodlike at low temperatures. (It should be noted, however, that this prediction using Mark's[25] RIS weights for st-PVC has not been experimentally verified, due to the unavailability of stereoregular PVC.)

Combining points 1 and 2, we can then explain the observed PRISM results as arising from a competition between "local openness" and chain stiffness. "Open" (but flexible) st-PMMA is *more* miscible with PVC than is the less open it-PMMA. On the other hand, stiff (although open) st-PVC is *less* miscible with PMMA than the more flexible it-PVC and at-PVC.

With respect to the above hypothesis, evidence from the pair distribution functions is inconclusive. Figure 6 shows $g_{VC-MMA}(r)$ for it-PVC blended with it-PMMA and st-PMMA at 250 K. Although the first peak in $g(r)$ is higher for it-PMMA, the second peak is more intense for st-PMMA. Integration of $g(r)$ shows that st-PMMA has a greater total number of nearest and next-nearest neighbor PVC sites than does it-PMMA, in spite of it-PMMA having a greater number of nearest neighbors. This result is qualitatively the same at other temperatures.

Conclusion

The results of this study can be summarized as follows:

(1) The known experimental trend is reproduced (st-PMMA is more miscible with PVC than is it-PMMA).

(2) The PRISM calculations predict a more pronounced shift in miscibility with PMMA tacticity for blends with it-PVC than with at-PVC or st-PVC.

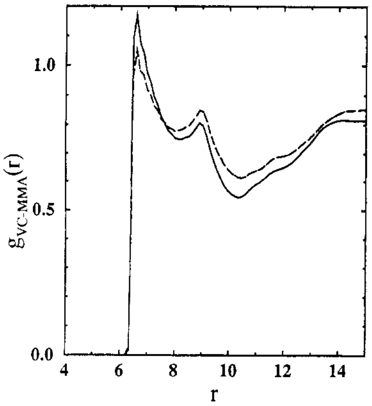

Figure 6. Calculated VC–MMA site–site pair distribution functions for isotactic PVC blended with isotactic (solid line) and syndiotactic (dashed line) PMMA. The temperature is 250 K.

(3) The calculations predict that st-PVC is less miscible with PMMA than is at-PVC or it-PVC.

(4) The tacticity effects seen here appear to be due to a competition between "local openness" and chain stiffness. Thus, stiff st-PVC is *less* miscible with PMMA, whereas "open" st-PMMA is *more* miscible with PVC.

(5) In the PRISM calculations, the miscibility differences with tacticity arise solely from conformational differences in the individual chains.

One of the strengths of PRISM theory is that it incorporates the effect of chain conformation on all length scales, from the scale of individual bonds up to the size of the chain. This means that whatever the important length scale(s) for a particular system, PRISM theory is able in principle to incorporate its effects. Both short- and intermediate-range effects appear to be relevant in determining the trends studied here. Other investigators have presented explanations of microstructure effects on miscibility in terms of local conformations or chain flexibility.[1,3,5,31] PRISM calculations allow these effects to be incorporated in a systematic fashion.

The model used in this study is admittedly coarse-grained. Its justification is primarily *a posteriori*: the level of detail was found adequate to give rise to the experimentally observed effect. It is straightforward to include more chemical detail in PRISM calculations, but this greatly increases the required computer time. (At the level of detail used here, a complete phase diagram can be calculated in about 2 h of CPU time on a Silicon Graphics Indigo workstation, once the $\hat{\omega}(k)$ functions have been computed.) The results from this study do not rule out factors other than chain conformational statistics contributing to tacticity effects in these and other systems.

PRISM theory accounts for the effects of intramolecular conformations on intermolecular structure. The effects of chain tacticity studied in this paper are fundamentally chain packing effects, or noncombinatorial contributions to the entropy of mixing, arising from differences in chain conformational statistics. These may also be described as free volume effects and presumably form part of the microscopic basis for the equation of state effects[11] in terms of which the experimental observations have been analyzed.[3]

References and Notes

(1) Schurer, J. W.; de Boer, A.; Challa, G. *Polymer* **1975**, *16*, 201.
(2) Vanderschueren, J.; Janssens, A.; Ladang, M.; Niezette, J. *Polymer* **1982**, *23*, 395.
(3) Vorenkamp, E. J.; ten Brinke, G.; Meijer, J. G.; Jager, H.; Challa, G. *Polymer* **1985**, *26*, 1725.
(4) Woo, E. M.; Barlow, J. W.; Paul, D. R. *J. Polym. Sci., Polym. Symp.* **1984**, *71*, 137.
(5) Lemieux, E.; Prud'homme, R. E.; Forte, R.; Jerome, R.; Teyssie, P. *Macromolecules* **1988**, *21*, 2148.
(6) Bernstein, R. E.; Cruz, C. A.; Paul, D. R.; Barlow, J. W. *Macromolecules* **1977**, *10*, 681.
(7) Roerdink, E.; Challa, G. *Polymer* **1978**, *19*, 173.
(8) Hashimoto, T.; Hasegawa, H. *Macromolecules* **1991**, *24*, 3443.
(9) Beaucage, G.; Stein, R. S.; Koningsveld, R. *Macromolecules* **1993**, *26*, 1603.
(10) Léonard, C.; Halary, J. L.; Monnerie, L. *Macromolecules* **1988**, *21*, 2988.
(11) Sanchez, I. C. *Polymer Compatibility and Incompatibility*; MMI Press Symposium Series; Šolc, K., Ed.; Harwood Academic Publishers: New York, 1982; Vol. 2, p 59.
(12) Schweizer, K. S.; Curro, J. G. *Phys. Rev. Lett.* **1987**, *58*, 246.
(13) Curro, J. G.; Schweizer, K. S. *Macromolecules* **1987**, *20*, 1928.
(14) Curro, J. G.; Schweizer, K. S. *J. Chem. Phys.* **1987**, *87*, 1842.
(15) Schweizer, K. S.; Curro, J. G. *J. Chem. Phys.* **1989**, *91*, 5059.
(16) Yoon, D. Y.; Flory, P. J. *Macromolecules* **1976**, *9*, 294.
(17) Chandler, D.; Andersen, H. C. *J. Chem. Phys.* **1972**, *57*, 1930.
(18) Curro, J. G.; Schweizer, K. S.; Grest, G. S.; Kremer, K. *J. Chem. Phys.* **1989**, *91*, 1357. Honnell, K. G.; Curro, J. G.; Schweizer, K. S. *Macromolecules* **1990**, *23*, 3496. Honnell, K. G.; McCoy, J. D.; Curro, J. G.; Schweizer, K. S.; Narten, A. H.; Habenschuss, A. *J. Chem. Phys.* **1991**, *94*, 4659.
(19) Deutsch, H.-P.; Binder, K. *Europhys. Lett.* **1992**, *17*, 697.
(20) Gehlsen, M. D.; Rosedale, J. H.; Bates, F. S.; Wignall, G. D.; Hansen, L.; Almadal, K. *Phys. Rev. Lett.* **1992**, *68*, 2452.
(21) Yethiraj, A.; Schweizer, K. S. *J. Chem. Phys.* **1992**, *97*, 5927; **1993**, *98*, 9080. Schweizer, K. S.; Yethiraj, A. *J. Chem. Phys.* **1993**, *98*, 9053.
(22) Honeycutt, J. D. *Polym. Prepr. (Am. Chem. Soc., Div. Polym. Chem.)* **1992**, *33* (1), 529.
(23) Lowden, L. J.; Chandler, D. *J. Chem. Phys.* **1973**, *59*, 6587; **1974**, *61*, 5228.
(24) Seitz, J. T. *J. Appl. Polym. Sci.* **1993**, *49*, 1331.
(25) Mark, J. E. *J. Chem. Phys.* **1972**, *56*, 451.
(26) Vacatello, M.; Flory, P. J. *Macromolecules* **1985**, *19*, 405.
(27) Brandrup, J.; Immergut, E. H., Eds. *Polymer Handbook*; Wiley: New York, 1989; p V-66.
(28) Schweizer, K. S.; Honnell, K. G.; Curro, J. G. *J. Chem. Phys.* **1992**, *96*, 3211. Melenkevitz, J.; Schweizer, K. S.; Curro, J. G. *Macromolecules* **1993**, *26*, 6190. Grayce, C. J.; Schweizer, K. S., preprint.
(29) A generalized Flory–Huggins theory was used to extract χ from experimental phase diagrams and to recalculate phase diagrams for the molecular weights used here. See: Mumby, S. J.; Sher, P. *Macromolecules* **1994**, *27*, 689.
(30) Flory, P. J. *Statistical Mechanics of Chain Molecules*; Hanser Publishers: Munich, 1989.
(31) Hsieh, D. T.; Peiffer, D. G.; Rabeony, M.; Siakali-Kioulafa, E.; Hadjichristidis, N. *Macromolecules* **1993**, *26*, 4978.